REVIEW ARTICLES

Solid-State Kinetic Models: Basics and Mathematical Fundamentals

Ammar Khawam and Douglas R. Flanagan*

Division of Pharmaceutics, College of Pharmacy, University of Iowa, Iowa City, Iowa 52242

Received: May 5, 2006; In Final Form: June 25, 2006

Many solid-state kinetic models have been developed in the past century. Some models were based on mechanistic grounds while others lacked theoretical justification and some were theoretically incorrect. Models currently used in solid-state kinetic studies are classified according to their mechanistic basis as nucleation, geometrical contraction, diffusion, and reaction order. This work summarizes commonly employed models and presents their mathematical development.

1. Introduction

Fifty years have passed since the publication of *Chemistry of the Solid State*, edited by W. E. Garner,[1] which covered theories of the solid state, including solid-state reaction kinetics. Jacobs and Tompkins[2] covered theories and derivations of some solid-state reaction models in Garner's text, specifically, nucleation and nuclei growth models. The derivation of these and other models has also appeared in Volume 22 of the *Chemical Kinetics Series* entitled, "Reactions in the Solid State" by Brown et al.[3] Later, Galwey and Brown[4] presented many of these same models. These and other older references are becoming less accessible because they have been out of print for many years. Researchers who seek the basis for these models and their mathematical foundations must find such old texts or access even older journal articles. Unfortunately, no single reference comprehensively presents the basics and mathematical development of these models. The lack of such a source causes authors to redundantly present reaction models in tabular form[5−10] as shown in Table 1. It is rare to find a solid-state kinetic report that does not list such reaction models because of the lack of a general source to which reference can be made.

This review is intended to provide a summary and mathematical basis for commonly used reaction models in solid-state kinetics.

2. Reaction Rate Laws

The rate of a solid-state reaction can be generally described by

$$\frac{d\alpha}{dt} = Ae^{-(E_a/RT)} f(\alpha) \tag{1}$$

where, A is the preexponential (frequency) factor, E_a is the activation energy, T is absolute temperature, R is the gas constant, $f(\alpha)$ is the reaction model, and α is the conversion fraction. For a gravimetric measurement, α is defined by

$$\alpha = \frac{m_0 - m_t}{m_0 - m_\infty} \tag{2}$$

where, m_0 is initial weight, m_t is weight at time t, and m_∞ is final weight.

Kinetic parameters (model, A, E_a) can be obtained from isothermal kinetic data by applying the above rate law (eq 1). Alternatively, eq 1 can be transformed into a nonisothermal rate expression describing reaction rate as a function of temperature at a constant heating rate by utilizing the following:

$$\frac{d\alpha}{dT} = \frac{d\alpha}{dt}\frac{dt}{dT} \tag{3}$$

where, $d\alpha/dT$ is the nonisothermal reaction rate, $d\alpha/dt$ is the isothermal reaction rate, and dT/dt is the heating rate (β). Substituting eq 1 into eq 3 gives the differential form of the nonisothermal rate law,

$$\frac{d\alpha}{dT} = \frac{A}{\beta}e^{-(E_a/RT)} f(\alpha) \tag{4}$$

Separating variables and integrating eqs 1 and 4 gives the integral forms of the isothermal and nonisothermal rate laws, respectively:

$$g(\alpha) = Ae^{-(E_a/RT)}\, t \tag{5}$$

and

$$g(\alpha) = \frac{A}{\beta}\int_0^T e^{-(E_a/RT)}\, dT \tag{6}$$

where, $g(\alpha)$ is the integral reaction model, defined by

$$g(\alpha) = \int_0^\alpha \frac{d\alpha}{f(\alpha)}$$

It should be noted that there is no consensus on the symbols used to represent these models, so the definitions of $f(\alpha)$ and

* Corresponding author: E-mail address: douglas-flanagan@uiowa.edu. Fax: (319) 335-9349.

10.1021/jp062746a CCC: $33.50
Published on Web 08/15/2006

Ammar M. N. Khawam received his B.S. in Pharmacy from the Jordan University of Science and Technology in 1997. After working in the pharmaceutical industry, he joined the graduate program at the University of Iowa and is completing his Ph.D. degree in Pharmaceutics. His research interests include physical properties of solids, drug stability, and thermal analysis applications to pharmaceutical development.

Douglas R. Flanagan received his B.S. in Pharmacy and M.S. and Ph.D. degrees in Pharmaceutical Chemistry, all from the University of Michigan. He has been on the faculty at the University of Connecticut and is presently Professor of Pharmaceutics at the University of Iowa. Dr. Flanagan's research interests include solid-state properties of drugs, diffusion and dissolution phenomena, controlled release formulation, and biodegradable polymeric systems.

$g(\alpha)$ may be reversed in some publications. Several reaction models ($f(\alpha)$ and $g(\alpha)$) are listed in Table 1.

Reaction kinetics in the solid-state are often studied by thermogravimetry, but they can also be studied by other analytical methods such as differential scanning calorimetry (DSC),[11,12] powder X-ray diffraction (PXRD),[13] and nuclear magnetic resonance (NMR).[14,15] For any analytical method, the measured parameter must be able to be transformed into a conversion fraction (α) that can be used in the kinetic equations.

Kinetic analysis (isothermal or nonisothermal) can be performed by either model-fitting or model-free (isoconversional) methods.[11] The use of isoconversional or model-free methods has increased recently[12,16−21] due to the ability of these methods to calculate E_a values without modelistic assumptions. However, such methods have some disadvantages,[22,23] and a reaction model is usually needed for a complete kinetic description of any solid-state reaction.[24] Different solid-state kinetic analysis methods have been recently reviewed.[11]

3. Models and Mechanisms in Solid-State Kinetics

A model is a theoretical, mathematical description of what occurs experimentally. In solid-state reactions, a model can describe a particular reaction type and translate that mathematically into a rate equation. Many models have been proposed in solid-state kinetics, and these models have been developed based on certain mechanistic assumptions. Other models are more empirically based, and their mathematics facilitates data analysis with little mechanistic meaning. Therefore, different rate expressions are produced from these models.

In homogeneous kinetics (e.g., gas or solution phases), kinetic studies are usually directed toward obtaining rate constants that can be used to describe the progress of a reaction. Additionally, the reaction mechanism is typically investigated and rate constant changes with temperature, pressure, or reactant/product concentrations are often helpful in uncovering mechanisms. These mechanisms involve to varying degrees the detailed

TABLE 1: Solid-State Rate and Integral Expressions for Different Reaction Models

model	differential form $f(\alpha) = 1/k\ d\alpha/dt$	integral form $g(\alpha) = kt$
	nucleation models	
power law (P2)	$2\alpha^{1/2}$	$\alpha^{1/2}$
power law (P3)	$3\alpha^{2/3}$	$\alpha^{1/3}$
power law (P4)	$4\alpha^{3/4}$	$\alpha^{1/4}$
Avrami−Erofeyev (A2)	$2(1-\alpha)[-\ln(1-\alpha)]^{1/2}$	$[-\ln(1-\alpha)]^{1/2}$
Avrami−Erofeyev (A3)	$3(1-\alpha)[-\ln(1-\alpha)]^{2/3}$	$[-\ln(1-\alpha)]^{1/3}$
Avrami−Erofeyev (A4)	$4(1-\alpha)[-\ln(1-\alpha)]^{3/4}$	$[-\ln(1-\alpha)]^{1/4}$
Prout−Tompkins (B1)	$\alpha(1-\alpha)$	$\ln[\alpha/(1-\alpha)] + c^a$
	geometrical contraction models	
contracting area (R2)	$2(1-\alpha)^{1/2}$	$1-(1-\alpha)^{1/2}$
contracting volume (R3)	$3(1-\alpha)^{2/3}$	$1-(1-\alpha)^{1/3}$
	diffusion models	
1-D diffusion (D1)	$1/(2\alpha)$	α^2
2-D diffusion (D2)	$-[1/\ln(1-\alpha)]$	$((1-\alpha)\ln(1-\alpha)) + \alpha$
3-D diffusion−Jander (D3)	$[3(1-\alpha)^{2/3}]/[2(1-(1-\alpha)^{1/3})]$	$(1-(1-\alpha)^{1/3})^2$
Ginstling−Brounshtein (D4)	$3/[2((1-\alpha)^{-1/3}-1)]$	$1-(2/3)\alpha-(1-\alpha)^{2/3}$
	reaction-order models	
zero-order (F0/R1)	1	α
first-order (F1)	$(1-\alpha)$	$-\ln(1-\alpha)$
second-order (F2)	$(1-\alpha)^2$	$[1/(1-\alpha)]-1$
third-order (F3)	$(1-\alpha)^3$	$(1/2)[(1-\alpha)^{-2}-1]$

[a] Constant of integration.

chemical steps by which a reactant is converted to product. However, in solid-state kinetics, mechanistic interpretations usually involve identifying a reasonable reaction model[25] because information about individual reaction steps is often difficult to obtain. However, the choice of a reaction model should ideally be supported by other complementary techniques such as microscopy, spectroscopy, X-ray diffraction, etc.[26]

4. Model Classification

Models are generally classified based on the graphical shape of their isothermal curves (α vs t or $d\alpha/dt$ vs α) or on their mechanistic assumptions. Based on their shape, kinetic models can be grouped into acceleratory, deceleratory, linear, or sigmoidal models (Figure 1). Acceleratory models are those in which the reaction rate ($d\alpha/dt$) is increasing (e.g., accelerating) as the reaction proceeds (Figure 1a); similarly, deceleratory reaction rates decrease with reaction progress (Figure 1b−d) while the rate remains constant for linear models (Figure 1e), and sigmoidal models show a bell-shaped relationship between rate and α (Figure 1f). Nonisothermally, α-temperature plots are not as distinctive in their shapes as they are isothermally. Figure 2 shows the nonisothermal α-temperature and $d\alpha/dT$ vs α plots generated using eqs 4 and 6. Models in Figures 1 and 2 can be displayed on a single graph using a reduced-time plot (isothermal data)[27] or a master plot method (for nonisothermal data).[7] These methods for graphical presentation are easy means of visually determining the most appropriate model for a particular data set.

Based on mechanistic assumptions, models are divided into nucleation, geometrical contraction, diffusion, or reaction-order (Table 1).

5. Model Derivation

Model derivation is based on several proposed reaction mechanisms which include nucleation, geometric shape, diffusion, and reaction order. Sestak and Berggren[28] have suggested a mathematical form that represents all models in a single general expression:

$$g(\alpha) = \alpha^m(1-\alpha)^n(-\ln(1-\alpha))^p \tag{7}$$

where m, n, and p are constants. By assigning values for these three variables, any model can be expressed. Derivations and theoretical implications of specific models are discussed below.

5.1. Nucleation and Nuclei Growth Models. The kinetics of many solid-state reactions have been described by nucleation models, specifically, the Avrami models. These reactions include crystallization,[29−31] crystallographic transition,[32] decomposition,[33,34] adsorption,[35,36] hydration,[37] and desolvation.[24] Skrdla and Robertson[38] have recently suggested a model that describes sigmoidal α-time curves based on the Maxwell−Boltzmann energy distribution and incorporates two rate constants: one for the acceleratory and one for the deceleratory region of the α-time curve.

5.1.1. Nucleation. Crystals have fluctuating local energies from imperfections due to impurities, surfaces, edges, dislocations, cracks, and point defects.[39] Such imperfections are sites for reaction nucleation since the reaction activation energy is minimized at these points. Thus, they are called, nucleation sites.[2,32]

A common reaction in solid-state kinetics follows the scheme:

$$A_{(s)} \rightarrow B_{(s)} + C_{(g)}$$

where, a solid "A" decomposes thermally to produce a solid "B" and gas "C".

Nucleation is the formation of a new product phase (B) at reactive points (nucleation sites) in the lattice of the reactant (A). Nucleation rates have been derived based on one of two assumptions:[2] nucleation is single- or multistepped (Table 2).

Single-step nucleation assumes that nucleation and nuclei growth occur in a single step. For N_0 potential nucleation sites (having equal nucleation probability), once the nuclei (N) are formed, they grow and the rate of nucleation is a simple first-order process according to

$$\frac{dN}{dt} = k_N(N_0 - N) \tag{8}$$

where, N is the number of growth nuclei present at time, t, and k_N is the nucleation rate constant. Separating variables and integrating eq 8 gives

$$N = N_0(1 - e^{-k_N t}) \tag{9}$$

Differentiation of eq 9 gives the exponential rate of nucleation:

$$\frac{dN}{dt} = k_N N_0 e^{-k_N t} \tag{10}$$

When k_N is small, the exponential term in eq 10 is $\sim$1 and the rate of nucleation is approximately constant, producing a linear rate of nucleation

$$\frac{dN}{dt} = k_N N_0 \tag{11}$$

However, when k_N is very large, the rate of nucleation is very high, indicating that all nucleation sites are rapidly or instantly nucleated producing an instantaneous rate of nucleation:

$$\frac{dN}{dt} = \infty \tag{12}$$

On the other hand, multistep nucleation assumes that several distinct steps are required to generate a growth nucleus.[40] Accordingly, formation of product B will induce strain within the lattice of A, rendering small aggregates of B unstable and causing them to revert back to reactant A. Strain can be overcome if a critical number (m_c) of B nuclei are formed. Therefore, two types of nuclei can be defined: germ and growth nuclei. A germ nucleus is submicroscopic with B particles below the critical number ($m < m_c$), which will either revert back to reactant A or grow to a growth nucleus, which is a nucleus with B particles exceeding the critical number ($m > m_c$) of particles allowing further reaction (i.e., nuclei growth). Therefore, a germ nucleus must accumulate a number of product molecules, "p", before it is converted to a growth nucleus. The rate constant (k_i) for addition of individual molecules in a nucleus up to p molecules (e.g., $n < p$) is assumed to be constant or $k_0 = k_1 = k_2 = k_3 = ... = k_{p-1} = k_i$ (i.e., rate constant for addition of each molecule). After p molecules have been accumulated (e.g., $n \geq p$), the rate constant (k_g) for further nucleus growth by addition of further molecules ($>p$) becomes, $k_p = k_{p+1} = k_{p+2} = k_{p+4} = ... = k_g$. It is assumed that the rate of nucleus growth is more than that of nucleus formation (i.e., $k_g > k_i$). Therefore, according to Bagdassarian,[40] if β successive events are necessary to form the growth nucleus, and each event

a.

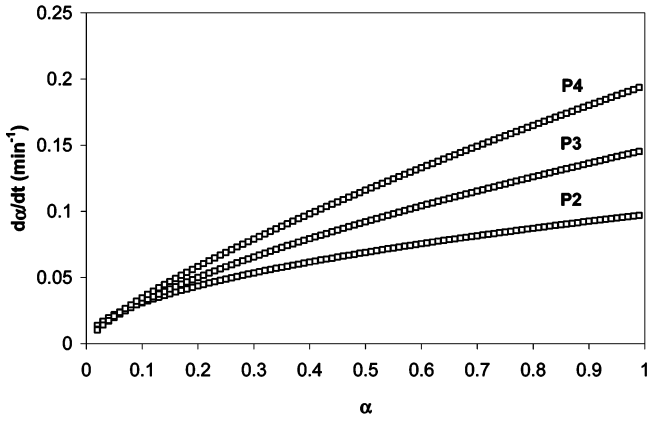
dα/dt (min-1)
α
P4
P3
P2

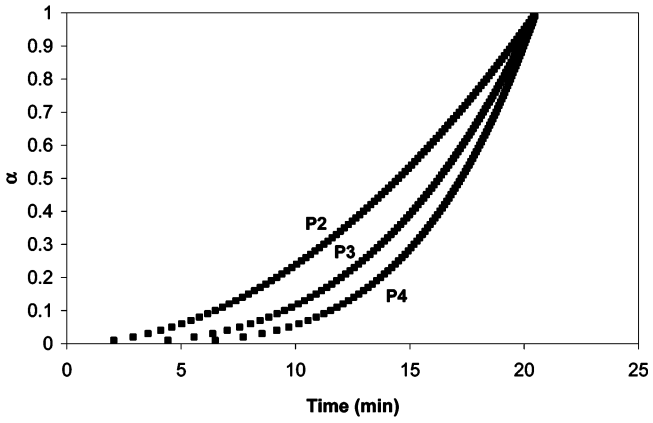
α
Time (min)
P2
P3
P4

b.

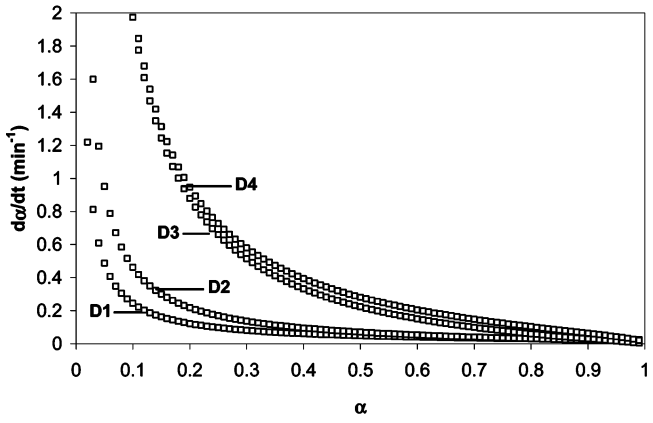
dα/dt (min-1)
α
D4
D3
D2
D1

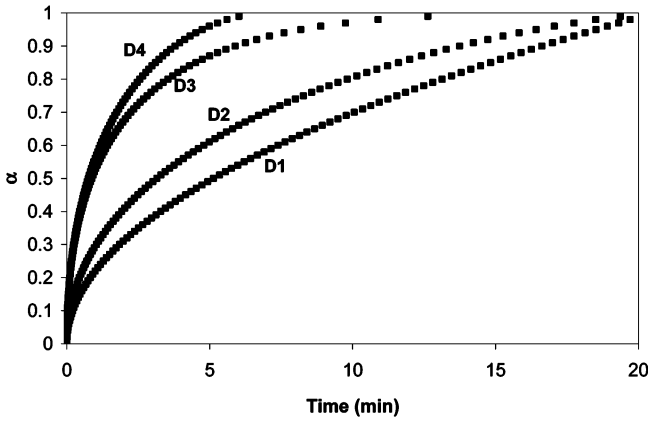
α
Time (min)
D4
D3
D2
D1

c.

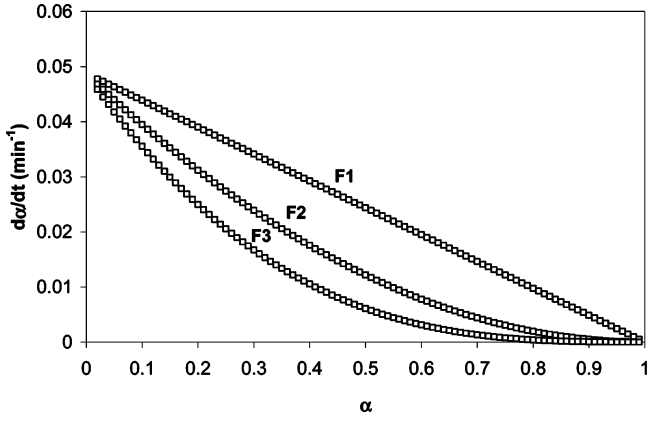
dα/dt (min-1)
α
F1
F2
F3

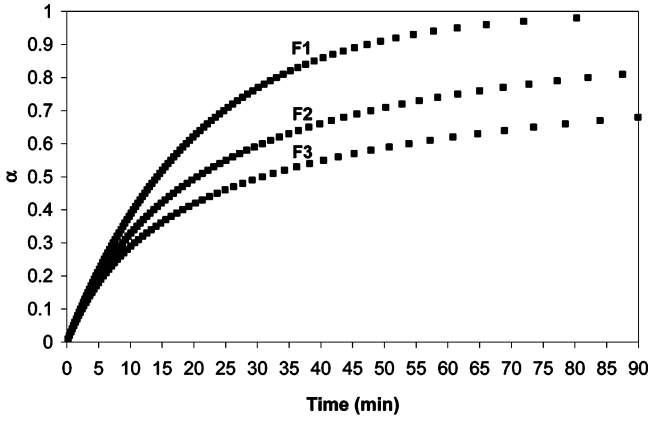
α
Time (min)
F1
F2
F3

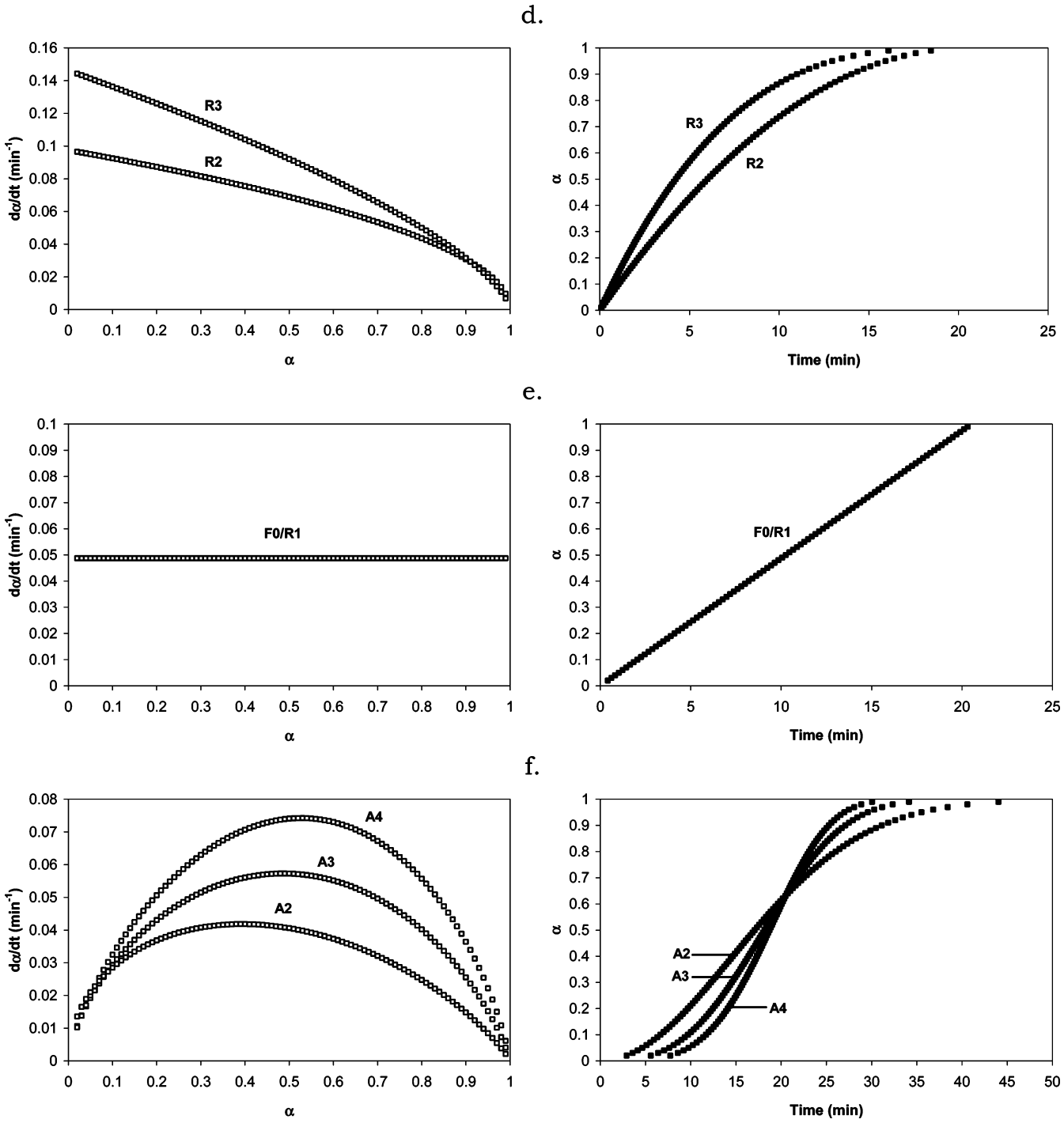

Figure 1. Isothermal dα/dt time and α time plots for solid-state reaction models (Table 1); data simulated with a rate constant of 0.049 min^{-1}: (a) acceleratory; (b−d) deceleratory; (e) constant; (f) sigmoidal.

has a probability equal to k_i, then the number of nuclei formed at time, t, is

$$N = \frac{N_0(k_i t)^\beta}{\beta!} = Dt^\beta \tag{13}$$

where, $D = N_0(k_i t)^\beta/\beta!$. After differentiation, eq 13 becomes

$$\frac{dN}{dt} = D\beta t^{\beta-1} \tag{14}$$

Equation 14 represents the power law of nucleation[2,40] (Table 2). Equation 14 was also derived by Allnatt and Jacobs,[41] but they assumed unequal rate constants for addition of successive molecules to the growth nuclei before reaching the critical size ($n = p$).

5.1.2. Nuclei Growth. The nuclei growth rate ($G(x)$) can be represented by the nuclei radius formed from growth. Nuclei growth rates usually vary with size.[2,4] For example, growth rates of small nuclei (often submicroscopic) would be different from that of large nuclei. Low growth rates are due to the instability of very small nuclei (germ nuclei), which revert to reactants. The radius of a stable nucleus (growth nucleus) at time, t,

a.

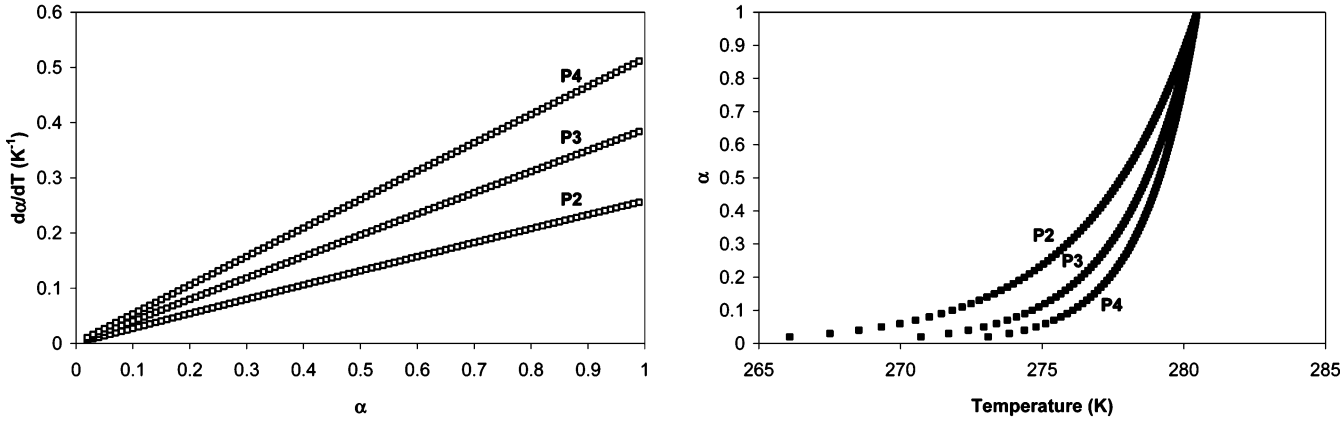
dα/dT (K⁻¹)
α
P4
P3
P2
Temperature (K)

b.

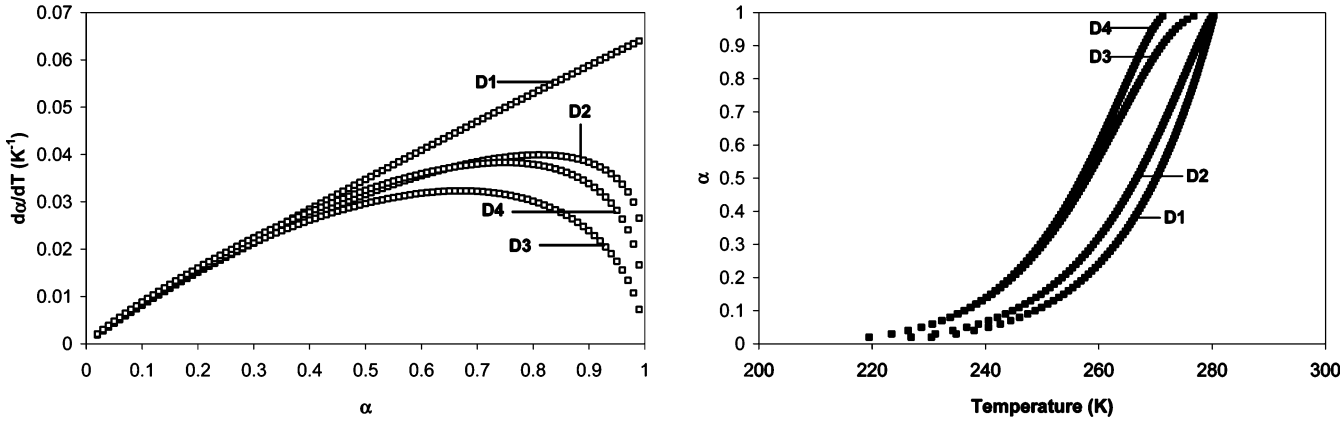
dα/dT (K⁻¹)
α
D1
D2
D4
D3
Temperature (K)

c.

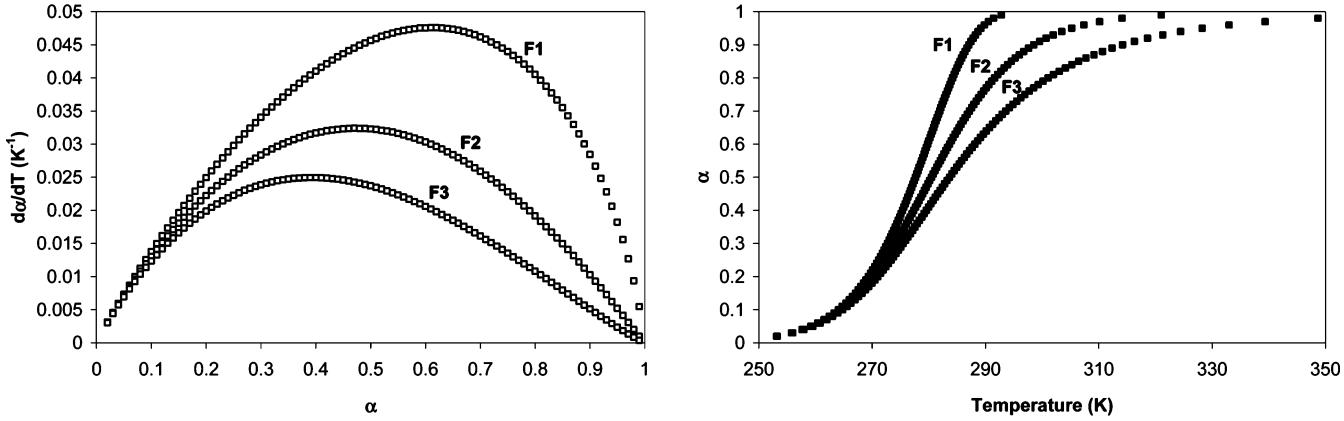
dα/dT (K⁻¹)
α
F1
F2
F3
Temperature (K)

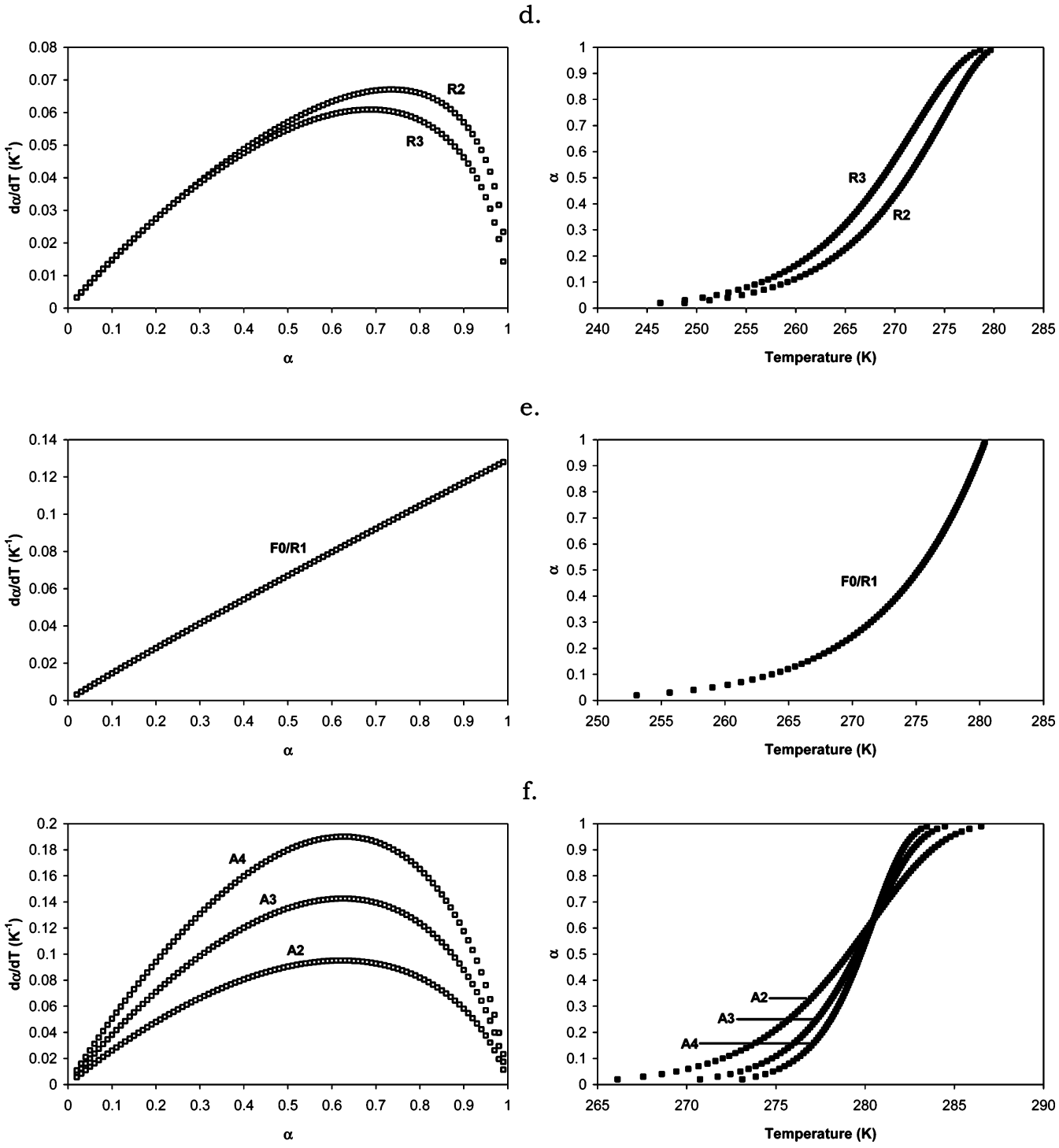

Figure 2. Nonisothermal dα/dT and α temperature plots for solid-state reaction models (Table 1); data simulated with a heating rate of 10 K/min, frequency factor of 1×10^{15} min^{-1}, and activation energy of 80 kJ/mol. (a) P-models; (b) D-models; (c−e) F and R models; (f) A-models.

($r(t,t_0)$), is

$$r(t,t_0) = \int_{t_0}^{t} G(x)\,\mathrm{d}x \tag{15}$$

where, $G(x)$ is the rate of nuclei growth and t_0 is the formation time of a growth nucleus.

In addition to nucleus radius, two important considerations in nuclei growth are also considered: nucleus shape (σ) and growth dimension (λ). When these are considered, they describe nuclei growth rate through the volume occupied by individual nuclei ($v(t)$). Therefore, a stable nucleus formed at time (t_0) occupies a volume $v(t)$ at time t according to

$$v(t) = \sigma[r(t,t_0)]^{\lambda} \tag{16}$$

where, λ is the number of growth dimensions (i.e., $\lambda = 1$, 2, or 3), σ is the shape factor (i.e., $4\pi/3$ for a sphere), and r is the radius of a nucleus at time t. Equation 16 gives the volume occupied by a single nucleus; the total volume occupied by all nuclei ($V(t)$) can be calculated by combining nucleation rate (dN/dt) and growth rate ($v(t,t_0)$) equations while accounting for different initial times of nucleus growth (t_0):

$$V(t) = \int_0^t v(t)\left(\frac{\mathrm{d}N}{\mathrm{d}t}\right)_{t=t_0} \mathrm{d}t_0 \tag{17}$$

TABLE 2: Mathematical Expressions for Nucleation Rates

nucleation rate law	differential form dN/dT	integral form N
exponential[a]	$k_N N_0 e^{-k_N t}$	$N_0(1 - e^{-k_N t})$
linear[a]	$k_N N_0$	$k_N N_0 t$
instantaneous[a]	∞	N_0
power[b]	$D\beta t^{\beta-1}$	Dt^{β}

[a] Single-step nucleation. [b] Multistep nucleation.

where, $V(t)$ is the volume of all growth nuclei and dN/dt is the nucleation rate. Substituting eq 15 into 16 and eq 16 into 17 gives

$$V(t) = \int_0^t \sigma\left(\int_{t_0}^t G(x)\,dx\right)^{\lambda} \left(\frac{dN}{dt}\right)_{t=t_0} dt_0 \tag{18}$$

The above equation may be integrated for any combination of nucleation and/or growth rate laws to give a rate expression of the form ($g(\alpha) = kt$) as listed in Table 1. However, this is not always possible since there is no functional relationship[4] between the nucleation and growth terms. Therefore, assumptions about nucleation (dN/dt) and growth ($v(t)$) rate equations must be made as described below.

5.1.3. Power Law (P) Models. For a simple case where nucleation rate follows the power law (eq 14) and nuclei growth is assumed constant ($G(x) = k_G$), eq 18 becomes

$$V(t) = \int_0^t \sigma(k_G(t - t_0))^{\lambda}(D\beta {t_0}^{\beta-1})\,dt_0 \tag{19}$$

Evaluating the integral in eq 19 gives[2]

$$V(t) = \sigma {k_G}^{\lambda} D\beta t^{\beta+\lambda}\left(1 - \frac{\lambda\beta}{\beta+1} + \frac{\lambda(\lambda-1)}{2!}\frac{\beta}{\beta+2}\ldots\right),\ \lambda \le 3 \tag{20}$$

If $D' = D\beta(1 - \lambda\beta/(\beta + 1) + \lambda(\lambda - 1)/2!\ \beta/(\beta + 2)...)$ and $n = \beta+\lambda$, eq 20 becomes

$$V(t) = \sigma {k_G}^{\lambda} D' t^n \tag{21}$$

Since, $V(t)$ is directly proportional to the reaction progress (α), α can be represented as

$$\alpha = V(t) \times C \tag{22}$$

where C is a constant equal to $1/V_0$ (V_0 initial volume). From eqs 21 and 22 we obtain

$$\alpha = \sigma {k_G}^{\lambda} C D' t^n \tag{23}$$

which can be rewritten as

$$\alpha = ((\sigma {k_G}^{\lambda} C D')^{1/n})^n t^n \tag{24}$$

If $k = (\sigma {k_G}^{\lambda} C D')^{1/n}$, eq 24 can be written as

$$\alpha = (kt)^n \tag{25}$$

Equation 25 can be rearranged to

$$(\alpha)^{1/n} = kt \tag{26}$$

Equation 26 represents the various power law (P) models (Table 1). Since these models assume constant nuclei growth without any consideration to growth restrictions (explained below), these models are usually applied to the analysis of the acceleratory period of a curve.

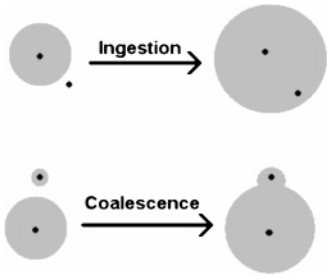

Figure 3. Two types of nuclei growth restrictions: black dots are nucleation sites; shaded areas are nuclei growth regions.

5.1.4. The Avrami−Erofeyev (A) Models. In any solid-state decomposition, there are certain restrictions on nuclei growth. Two such restrictions have been identified[4] (Figure 3). (a) Ingestion − elimination of a potential nucleation site by growth of an existing nucleus; ingested sites never produce a growth nucleus due to their inclusion in a growth nucleus. Ingested nuclei are called "phantom" nuclei. (b) Coalescence − loss of reactant/product interface when reaction zones of two or more growing nuclei merge.

An expression relating the number of nuclei sites is[42]

$$N_1(t) = N_0 - N(t) - N_2(t) \tag{27}$$

where N_0 is the total number of possible nuclei-forming sites, $N_1(t)$ is the actual number of nuclei at time t, $N_2(t)$ is the number of nuclei ingested, and $N(t)$ is the number of nuclei activated (i.e., developed into growth nuclei). From eq 27, a nucleation rate (dN/dt) known as the modified exponential law can be developed.[2] However, if this nucleation rate is substituted into eq 17, the resulting expression does not have an analytical solution.[2] To deal with this issue, an extended conversion fraction (α') was proposed,[43] which is the conversion fraction previously defined in eq 25 ($\alpha = [kt]^n$) that neglects ingestion (i.e., accounts for active and phantom nuclei) and nuclei coalescence. Therefore, $\alpha' \ge \alpha$. Values of α can be evaluated by determining their relation to values of α'.

The extended conversion fraction (α') was related to the actual conversion fraction (α) by Avrami[44] who obtained

$$d\alpha' = \frac{d\alpha}{(1 - \alpha)} \tag{28}$$

which, upon integration, gives

$$\alpha' = -\ln(1 - \alpha) \tag{29}$$

Substituting the value of (α') from eq 25 into eq 29 gives

$$(kt)^n = -\ln(1 - \alpha) \tag{30}$$

which can be rearranged to

$$[-\ln(1 - \alpha)]^{1/n} = kt \tag{31}$$

Erofeyev (Erofe'ev or Erofeev)[45] followed a different approach to derive a special case of eq 31 for $n = 3$. Therefore, eq 31 was attributed to both Avrami and Erofeyev and represents different Avrami−Erofeyev (A) models (Table 1) for different values of n. These "A" models are also called the JMAEK models, which stands for Johnson, Mehl, Avrami, Erofeyev, and Kholmogorov, in recognition of the researchers that have contributed to their development.[4]

5.1.5. Autocatalytic Models. In homogeneous kinetics, autocatalysis occurs when the products catalyze the reaction; this occurs when the reactants are regenerated during a reaction in what is called "branching". The reactants will eventually be consumed and the reaction will enter a "termination" stage where it will cease. A similar observation can be seen in solid-state kinetics. Autocatalysis occurs in solid-state kinetics if nuclei growth promotes continued reaction due to the formation of imperfections such as dislocations or cracks at the reaction interface (i.e., branching). Termination occurs when the reaction begins to spread into material that has decomposed.[46] Prout and Tompkins[47] derived an autocatalysis model (B1) for the thermal decomposition of potassium permanganate which produced considerable crystal cracking during decomposition.

In autocatalytic reactions, the nucleation rate can be defined by

$$\frac{dN}{dt} = k_N N_0 + (k_B - k_T)N \tag{32}$$

where, k_B is the branching rate constant and k_T is the termination rate constant. If $k_N N_0$ is neglected, eq 32 becomes

$$\frac{dN}{dt} = (k_B - k_T)N \tag{33}$$

This could occur in one of two cases: (1) k_N is very large so that initial nucleation sites are depleted rapidly and calculations of dN/dt are valid for time intervals after N_0 sites are depleted. (2) k_N is very small so that $k_N N_0$ can be ignored.

The reaction rate is related to number of nuclei by

$$\frac{d\alpha}{dt} = k'N \tag{34}$$

where, k' is the reaction rate constant. Prout and Tompkins found that the shape of α vs time plots for the degradation of potassium permanganate was sigmoidal. Therefore, an inflection point exists (α_i, t_i) at which dN/dt will change signs. From the boundary conditions that need to be satisfied at that inflection point (i.e., $k_B = k_T$), the following can be defined:

$$k_T = k_B\left(\frac{\alpha}{\alpha_i}\right) \tag{35}$$

Substituting eq 35 into eq 33 gives

$$\frac{dN}{dt} = k_B\left(1 - \frac{\alpha}{\alpha_i}\right)N \tag{36}$$

Since $dN/d\alpha = dN/dt \cdot dt/d\alpha$, eq 37 can be obtained:

$$\frac{dN}{d\alpha} = k''\left(1 - \frac{\alpha}{\alpha_i}\right) \tag{37}$$

where $k'' = k_B/k'$. Assuming k_B is independent of α, separating variables in eq 37 and integrating gives

$$N = k''\left(\alpha - \frac{\alpha^2}{2\alpha_i}\right) \tag{38}$$

Substituting eq 38 into 34 gives

$$\frac{d\alpha}{dt} = k_B\left(\alpha - \frac{\alpha^2}{2\alpha_i}\right) \tag{39}$$

Since Prout and Tompkins assumed that $\alpha_i = 0.5$, eq 39 reduces to

$$\frac{d\alpha}{dt} = k_B\alpha(1 - \alpha) \tag{40}$$

Separating variables and integrating eq 40 gives

$$\ln\frac{\alpha}{1 - \alpha} = k_B t + c \tag{41}$$

where c is the integration constant.

Equation 41 is the Prout−Tompkins (B1) model (Table 1) which well fits the thermal degradation of solid potassium permanganate. It should be noted that, unlike other models, the integration of eq 40 was performed without limits, simply because with a lower limit ($\alpha = 0$), the value is negative infinity. As a result, the integration constant appears in the Prout−Tompkins equation (eq 41). One of the limitations in some literature on this equation is that it is reported without the constant term as

$$\ln\frac{\alpha}{1 - \alpha} = k_B t \tag{42}$$

This causes confusion since eq 42 will give negative time values for $\alpha < 0.5$ (Figure 4). To overcome this problem, an integration constant, c, in eq 41 is needed which shifts the curve toward positive time values. There is no general criterion for what the integration constant should be; however, Prout and Tompkins used t_{max}, which is the time needed for the maximum rate (i.e., the inflection point) and which is approximately the same as $t_{1/2}$ used by Carstensen.[48] We have used a time equivalent to $\alpha = 0.01$ (30.21 min) for our simulation (Figure 4), but other values would be equally valid.

The Prout−Tompkins model has been criticized because of the assumptions required for its derivation; other forms of it have been proposed.[46,49−51] Skrdla[52] considered nucleation and branching as two separate processes (independent but coupled) having two different rate constants and proposed an autocatalytic rate expression. The proposed expression gives the Prout−Tompkins model if the nucleation and branching rate constants are equal.[52] Guinesi et al.[53] have shown that titanium(IV)−EDTA decarboxylates in two steps, the first being the B1 model while the second is the R3 model.

5.2. Geometrical Contraction (R) Models. These models assume that nucleation occurs rapidly on the surface of the crystal. The rate of degradation is controlled by the resulting reaction interface progress toward the center of the crystal. Depending on crystal shape, different mathematical models may be derived. For any crystal particle the following relation is applicable:

$$r = r_0 - kt \tag{43}$$

where r is the radius at time t, r_0 is the radius at time t_0, and k is the reaction rate constant. If a solid particle is assumed to have cylindrical or spherical/cubical shapes (Figure 5), the contracting cylinder (contracting area) or contracting sphere/cube (contracting volume) models,[54] respectively, can be derived. Dehydration of calcium oxalate monohydrate was shown to follow geometrical contraction models.[55−57]

5.2.1. The Contracting Cylinder (Contracting Area) Model − R2. For a cylindrical solid particle, the volume is $h\pi r^2$, where h is the cylinder height and r is the cylinder radius. For "n" particles, the volume is $nh\pi r^2$. Since, weight = volume ×

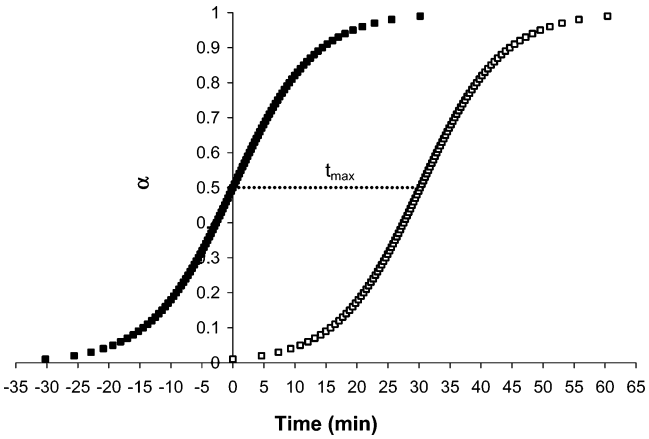

Figure 4. Isothermal α time plots for the Prout−Tompkins reaction model (Table 1); data simulated with a rate constant of 0.152 min^{-1}: (■) data simulated according to eq 42; (□) data simulated according to eq 41 where $c = t_{max}$ (30.21 min).

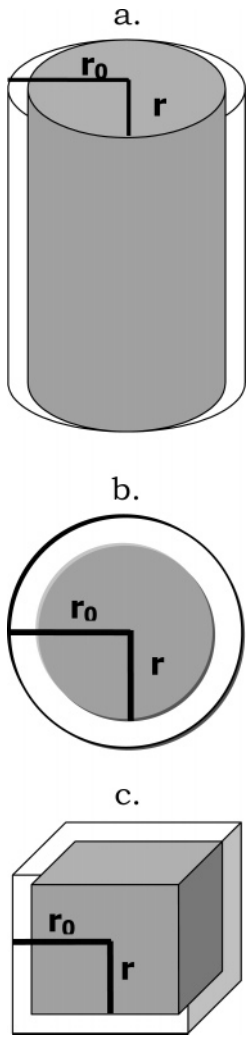

Figure 5. Geometrical crystal shapes: (a) cylinder; (b) sphere; (c) cube.

density (ρ), the weight of "n" cylindrical particles is $n\rho h\pi r^2$. From the earlier definition of conversion fraction (α, eq 2) and assuming $m_\infty \approx 0$, we obtain

$$\alpha = \frac{m_0 - m_t}{m_0} \tag{44}$$

Therefore, for n reacting particles:

$$\alpha = \frac{n\rho h\pi r_0^{\,2} - n\rho h\pi r^2}{n\rho h\pi r_0^{\,2}} \tag{45}$$

Equation 45 reduces to

$$\alpha = \left(1 - \frac{r^{\,2}}{r_0^{\,2}}\right) \tag{46}$$

Substituting the value of r from eq 43 gives

$$\alpha = 1 - \left(\frac{r_0 - kt}{r_0}\right)^2 \tag{47}$$

which can be rearranged to

$$1 - \alpha = \left(1 - \frac{k}{r_0}t\right)^2 \tag{48}$$

If $k_o = k/r_0$, eq 48 becomes the contracting cylinder model:

$$1 - (1 - \alpha)^{1/2} = k_o t \tag{49}$$

5.2.2. The Contracting Sphere/Cube (Contracting Volume) Model − R3. If a solid particle has a spherical or cubical shape, a contracting sphere/cube model can be derived. A sphere has a volume of $4\pi r^3/3$. For n particles, the volume is $4n\pi r^3/3$. Since weight = volume × density (ρ), the weight of n spherical particles is

$$\text{weight} = \frac{4}{3}n\rho\pi r^3 \tag{50}$$

Equation 44, for a reaction involving n particles becomes

$$\alpha = \frac{\frac{4}{3}n\rho\pi r_0^{\,3} - \frac{4}{3}n\rho\pi r^3}{\frac{4}{3}n\rho\pi r_0^{\,3}} \tag{51}$$

which reduces to

$$\alpha = \left(1 - \frac{r^3}{r_0^{\,3}}\right) \tag{52}$$

Substituting for r from eq 43 gives

$$\alpha = 1 - \left(\frac{r_0 - kt}{r_0}\right)^3 \tag{53}$$

which can be rearranged to

$$1 - \alpha = \left(1 - \frac{k}{r_0}t\right)^3 \tag{54}$$

If $k_o = k/r_0$, eq 54 becomes the contracting sphere model as

$$1 - (1 - \alpha)^{1/3} = k_o t \tag{55}$$

A similar approach for cubic crystals leads to the same general expression. It should be emphasized that particle size is incorporated in the rate constant (k) for these models and for other models where geometry of the solid crystal is part of the mathematical derivation (e.g., diffusion models). Therefore, a sample of varying particle size will have variable reaction rate

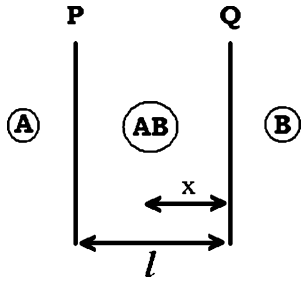

Figure 6. One-dimensional diffusion through a flat plane.[62] A and B are reactants, AB is the product interface, l is the thickness of the interface AB, and x is the distance measured from interface Q into AB.

constants, which will cause α-time or α-temperature curves to shift. This would produce a curved isoconversional plot if an isoconversional method is used for kinetic analysis;[22,23] sieving the solid sample will greatly reduce this effect. Particle size effects on the shape of α-time/temperature plots has been described by Koga and Criado.[58,59]

5.3. Diffusion (D) Models. One of the major differences between homogeneous and heterogeneous kinetics is the mobility of constituents in the system. While reactant molecules are usually readily available to one another in homogeneous systems, solid-state reactions often occur between crystal lattices or with molecules that must permeate into lattices where motion is restricted and may depend on lattice defects.[60] A product layer may increase where the reaction rate is controlled by the movement of the reactants to or products from the reaction interface. Solid-state reactions are not usually controlled by mass transfer except for a few reversible reactions or when large evolution or consumption of heat occurs. Diffusion usually plays a role in the rates of reaction between two reacting solids, when reactants are in separate crystal lattices.[3] Wyandt and Flanagan[61] have shown that desolvation of sulfonamide-ammonia adducts follows diffusion models. A correlation was found between calculated desolvation activation energies of the ammonia adducts and the sulfonamide's intrinsic acidity. This finding was attributed to an acid−base-type interaction between the sulfonamide (acid) and ammonia (base) in the solid state. The pK_a of the drug was found to inversely relate to the strength of the ammonia−drug interaction, which in turn affected desolvation activation energy.

In diffusion-controlled reactions, the rate of product formation decreases proportionally with the thickness of the product barrier layer. For metallic oxidation, this involves a moving boundary and is considered a "tarnishing reaction"[60,62] which is depicted in Figure 6. According to Figure 6, the mass of B moving across P (unit area) in time, dt, to form product AB is

$$\frac{\mathrm{d}l}{\mathrm{d}t} = -D\frac{M_{\mathrm{AB}}}{M_{\mathrm{B}}\rho}\frac{\mathrm{d}C}{\mathrm{d}x} \tag{56}$$

where, M_{AB} and M_{B} are the molecular weights of AB and B, respectively, D is the diffusion coefficient, ρ is the density of the product (AB), l is the thickness of the product layer (AB), C is the concentration of B in AB, and x is the distance from interface Q into AB. Assuming a linear concentration gradient of B in AB, $\mathrm{d}C/\mathrm{d}x|_{x=l} = -(C_2 - C_1)/l$, where C_2 and C_1 are the concentrations of B at interfaces P and Q, respectively, eq 56 becomes

$$\frac{\mathrm{d}l}{\mathrm{d}t} = D\frac{M_{\mathrm{AB}}}{M_{\mathrm{B}}\rho}\frac{(C_2 - C_1)}{l} \tag{57}$$

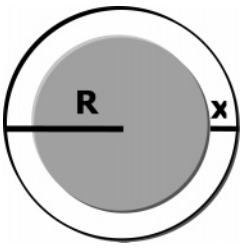

Figure 7. Schematic representation of a spherical particle reaction.

Separating variables and integrating eq 57 gives

$$l^2 = 2\mathrm{D}\frac{M_{\mathrm{AB}}(C_2 - C_1)}{M_{\mathrm{B}}\rho}t \tag{58}$$

If $k = 2D[M_{\mathrm{AB}}(C_2 - C_1)]/M_{\mathrm{B}}\rho$, eq 58 becomes

$$l^2 = kt \tag{59}$$

Equation 59 is known as the parabolic law.[62] The simplest rate equation is for an infinite flat plane that does not involve a shape factor (e.g., one-dimensional), where the conversion fraction (α) is directly proportional to product layer thickness, "l". Therefore, eq 59 becomes

$$\alpha^2 = k't \tag{60}$$

where k' is a constant. Equation 60 represents the one-dimensional diffusion (D1) model.

The three-dimensional diffusional (D3) model is based on the assumption of spherical solid particles (Figure 7). The conversion fraction for a reaction involving n spherical particles using eqs 44 and 50 is

$$\alpha = \frac{\frac{4}{3}n\rho\pi R^3 - \frac{4}{3}n\rho\pi(R - x)^3}{\frac{4}{3}n\rho\pi R^3} \tag{61}$$

where x is the thickness of the reaction zone. Upon simplification, eq 61 becomes

$$\alpha = 1 - \left(\frac{R - x}{R}\right)^3 \tag{62}$$

Equation 62 can be rearranged to

$$x = R(1 - (1 - \alpha)^{1/3}) \tag{63}$$

Jander[63] used the parabolic law (eq 59) to define x. Therefore, subsitituing eq 63 (after squaring x) into eq 59 gives

$$R^2(1 - (1 - \alpha)^{1/3})^2 = kt \tag{64}$$

Assuming $k' = k/R^2$, eq 64 becomes the D3 (Jander) model:

$$(1 - (1 - \alpha)^{1/3})^2 = k't \tag{65}$$

Ginstling−Brounshtein have shown[64] that the Jander model (eq 65) which used the parabolic law (derived for a plane surface) is oversimplified and holds only at low conversion values (i.e., low x/R values). The steady-state solution of Fick's first law for radial diffusion in a sphere is[65]

$$C_{(r)} = \frac{aC_1(b - r) + bC_2(r - a)}{r(b - a)} \tag{66}$$

where $C(r)$ is the reactant concentration at a particular value of r ($a < r < b$), C_1 is the concentration of the diffusing species at surface $r = a$, and C_2 is the concentration of the diffusing species at surface $r = b$. The reaction at the interface is assumed to occur at a much faster rate than diffusion, therefore, $C_1 \approx 0$. Therefore, eq 66 becomes

$$C_{(r)} = \frac{bC_2(r-a)}{r(b-a)} \tag{67}$$

Taking the derivative of the above equation with respect to r at $r = a$ gives

$$\frac{dC}{dr}|_{r=a} = \frac{(b-a)bC_2}{a(b-a)^2} \tag{68}$$

According to Figure 7, $a = R-x$ and $b = R$, so that eq 68 becomes

$$\frac{dC}{dr} = \frac{RC_2}{(R-x)x} \tag{69}$$

The rate of reaction zone advance, dx/dt, can be related to dC/dr by[64]

$$\frac{dx}{dt} = \frac{D}{\epsilon}\frac{dC}{dr} \tag{70}$$

where D is the diffusion coefficient, ϵ is a proportionality constant equal to $\rho n/\mu$ (ρ and μ are the specific gravity and molecular weight of the product, respectively, and n is the stoichiometric coefficient of the reaction). Subsituting eq 69 into eq 70 gives

$$\frac{dx}{dt} = \frac{D}{\epsilon}\frac{RC_2}{(R-x)x} \tag{71}$$

which can be rewritten as

$$\frac{dx}{dt} = k\frac{R}{(Rx-x^2)} \tag{72}$$

where $k = DC_2/\epsilon$. Separating variables and integrating eq 72 gives

$$x^2\left(\frac{1}{2} - \frac{x}{3R}\right) = kt \tag{73}$$

Substituting for x in eq 73 with the value of x in eq 63 and rearranging gives

$$1 - \frac{2}{3}\alpha - (1-\alpha)^{2/3} = kt \tag{74}$$

Equation 74 is the Ginstling−Brounshtein (D4) model. The D4 model is another type of three-dimensional model. Buscaglia and Milanese[66] have proposed a generalized form of the Ginstling−Brounshtein model and have discussed limitations related to the boundary conditions for this model. The reaction between manganese oxide (Mn_3O_4) and sodium carbonate was shown to follow the D4 model.[67]

If solid particles are assumed to be cylindrical, and diffusion occurs radially through a cylindrical shell with an increasing reaction zone, a two-dimensional diffusion (D2) model can be derived. The D2 model can be derived using the same general approach used for the D3 model. For a cylindrical particle, eq 63 is defined as

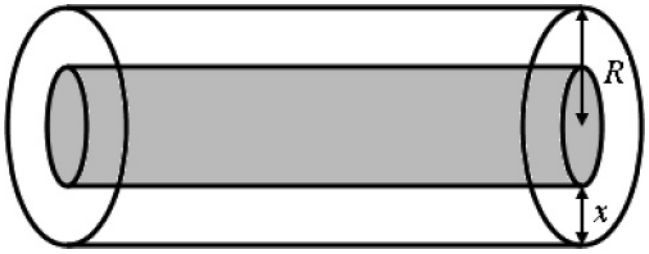

Figure 8. Schematic representation of a cylindrical particle reaction.

$$x = R(1-(1-\alpha)^{1/2}) \tag{75}$$

If Jander's approach is followed, the resulting equation is

$$(1-(1-\alpha)^{1/2})^2 = k't \tag{76}$$

where, $k' = k/R^2$. Equation 76 is not the D2 model usually cited in the literature. The usual D2 model is derived following the Ginstling−Brounshtein approach. The steady-state solution of Fick's first law for radial diffusion in a cylinder is[68]

$$C_{(r)} = \frac{C_1\ln(b/r) + C_2\ln(r/a)}{\ln(b/a)} \tag{77}$$

where $C(r)$ is the reactant concentration at a particular value of r ($a < r < b$), C_1 is the concentration of the diffusing species at surface $r = a$, and C_2 is the concentration of the diffusing species at surface $r = b$. The reaction at the interface is assumed to occur at a much faster rate than diffusion, making $C_1 \approx 0$. Therefore, eq 77 becomes

$$C_{(r)} = \frac{C_2\ln(r/a)}{\ln(b/a)} \tag{78}$$

Taking the derivative of the above equation with respect to r at $r = a$ gives

$$\frac{dC}{dr}|_{r=a} = \frac{C_2}{a\ln(b/a)} \tag{79}$$

According to Figure 8, $a = R-x$ and $b = R$, therefore, eq 79 becomes

$$\frac{dC}{dr} = \frac{C_2}{(R-x)\ln(R/(R-x))} \tag{80}$$

Subsituting eq 80 into 70 gives

$$\frac{dx}{dt} = \frac{k}{(R-x)\ln(R/(R-x))} \tag{81}$$

where $k = DC_2/\epsilon$. Substituting for the value of x in eq 81 with x from eq 75 and rearranging gives

$$\frac{dx}{dt} = -\frac{k}{(1-\alpha)^{1/2}\ln(1-\alpha)^{1/2}} \tag{82}$$

The derivative of eq 75 is

$$dx = \frac{R}{2(1-\alpha)^{1/2}}d\alpha \tag{83}$$

Substituting eq 83 into eq 82 and rearranging gives

$$\frac{d\alpha}{dt} = -\frac{k'}{\ln(1-\alpha)} \tag{84}$$

where $k' = 4k/R^2$. Equation 84 is the differential form of the D2 model. The integral form (Table 1) of the D2 model can be obtained by separating variables and integrating eq 84.

Finally, JMAEK models ($(-\ln[1-\alpha])^{1/n} = kt$) have been modified to account for diffusion[69] where n becomes 1.5 (one-dimension), 2 (two-dimensions), and 2.5 (three-dimensions); the diffusion coefficient (D) is included in the reaction rate constant (k).

5.4. Order-Based (F) Models. Order-based models are the simplest models as they are similar to those used in homogeneous kinetics. In these models, the reaction rate is proportional to concentration, amount or fraction remaining of reactant(s) raised to a particular power (integral or fractional) which is the reaction order. Some kinetic analysis methods force data into an order-based model that may not be appropriate.[4,27] Order-based models are derived from the following general equation

$$\frac{d\alpha}{dt} = k(1-\alpha)^n \tag{85}$$

where $d\alpha/dt$ is the rate of reaction, k is the rate constant, and n is the reaction order.

If $n = 0$ in eq 85, the zero-order model (F0/R1) model is obtained and eq 85 becomes

$$\frac{d\alpha}{dt} = k \tag{86}$$

After separating variables and integrating, eq 86 becomes

$$\alpha = kt \tag{87}$$

If $n = 1$ in eq 85, the first-order model (F1) model is obtained and eq 85 becomes

$$\frac{d\alpha}{dt} = k(1-\alpha) \tag{88}$$

Separating variables and integrating eq 88 leads to the first-order integral expression

$$-\ln(1-\alpha) = kt \tag{89}$$

The first-order model, also called the Mampel model,[70,71] is a special case of the Avrami−Erofeyev (A) models where $n = 1$. Similarly, second-order ($n = 2$) and third-order ($n = 3$) models can be obtained (Table 1). Lopes et al.[72] have shown that decomposition of gadolinium(III) complexes follows a zero-order model. Thermal oxidation of porous silicon[73] and desorption of 2-phenylethylamine (PEA) from silica surfaces[74] were shown to follow a first-order model.

6. Summary

We have attempted to summarize the assumptions and mathematical derivation of the most commonly used reaction models in solid-state kinetics. This review has not been exhaustive but rather representative of the common models used. Hopefully our presentation is a useful pedagogic tool for understanding solid-state kinetic models. Even though we have focused on reactions involving weight loss ($A_{(s)} \rightarrow B_{(s)} + C_{(g)}$), many of the models are applicable to other solid-state reactions where, for example, evolution or consumption of heat is measured. We hope that this work has demonstrated that solid-state kinetic models have a theoretical physical meaning and are not merely based on goodness of data fits to complex mathematical expressions.

Finally, investigators are challenged to better understand the models and mathematical tools they apply to solid-state kinetic reactions. We hope our work helps resolve some of the lack of understanding of solid-state kinetic models.

References and Notes

(1) *Chemistry of the solid state*; Garner, W. E., Ed.; Academic Press: New York, 1955.
(2) Jacobs, P. W. M.; Tompkins, F. C. Classification and theory of solid reactions. In *Chemistry of the solid state*; Garner, W. E., Ed.; Academic Press: New York, 1955; Chapter 7.
(3) Brown, M. E.; Dollimore, D.; Galwey, A. K. Reactions in the solid state. In *Comprehensive chemical kinetics*; Bamford, C. H., Tipper, C. F. H., Eds.; Elsevier: Amsterdam, 1980; Vol. 22, Chapter 3.
(4) Galwey, A. K.; Brown, M. E. *Thermal decomposition of ionic solids: Chemical properties and reactivities of ionic crystalline phases*; Elsevier: Amsterdam, 1999; Chapter 3.
(5) Zhou, D. L.; Grant, D. J. W. *J. Phys. Chem. A* **2004**, *108*, 4239.
(6) Perez-Maqueda, L. A.; Criado, J. M.; Gotor, F. J.; Malek, J. *J. Phys. Chem. A* **2002**, *106*, 2862.
(7) Gotor, F. J.; Criado, J. M.; Malek, J.; Koga, N. *J. Phys. Chem. A* **2000**, *104*, 10777.
(8) MacNeil, D. D.; Dahn, J. R. *J. Phys. Chem. A* **2001**, *105*, 4430.
(9) Alkhamis, K. A.; Salem, M. S.; Obaidat, R. M. *J. Pharm. Sci.* **2006**, *95*, 859.
(10) Capart, R.; Khezami, L.; Burnham, A. K. *Thermochim. Acta* **2004**, *417*, 79.
(11) Khawam, A.; Flanagan, D. R. *J. Pharm. Sci.* **2006**, *95*, 472.
(12) Vyazovkin, S.; Dranca, I. *J. Phys. Chem. B* **2005**, *109*, 18637.
(13) Kirsch, B. L.; Richman, E. K.; Riley, A. E.; Tolbert, S. H. *J. Phys. Chem. B* **2004**, *108*, 12698.
(14) Jones, A. R.; Winter, R.; Florian, P.; Massiot, D. *J. Phys. Chem. B* **2005**, *109*, 4324.
(15) Bertmer, M.; Nieuwendaal, R. C.; Barnes, A. B.; Hayes, S. E. *J. Phys. Chem. B* **2006**, *110*, 6270.
(16) Yu, Y. F.; Wang, M. H.; Gan, W. J.; Tao, Q. S.; Li, S. J. *J. Phys. Chem. B* **2004**, *108*, 6208.
(17) Premkumar, T.; Govindarajan, S.; Coles, A. E.; Wight, C. A. *J. Phys. Chem. B* **2005**, *109*, 6126.
(18) Bendall, J. S.; Ilie, A.; Welland, M. E.; Sloan, J.; Green, M. L. H. *J. Phys. Chem. B* **2006**, *110*, 6569.
(19) Vyazovkin, S.; Dranca, I. *J. Phys. Chem. B* **2004**, *108*, 11981.
(20) Vyazovkin, S.; Dranca, I.; Fan, X. W.; Advincula, R. *J. Phys. Chem. B* **2004**, *108*, 11672.
(21) Milev, A. S.; McCutcheon, A.; Kannangara, G. S. K.; Wilson, M. A.; Bandara, T. Y. *J. Phys. Chem. B* **2005**, *109*, 17304.
(22) Khawam, A.; Flanagan, D. R. *Thermochim. Acta* **2005**, *436*, 101.
(23) Khawam, A.; Flanagan, D. R. *Thermochim. Acta* **2005**, *429*, 93.
(24) Khawam, A.; Flanagan, D. R. *J. Phys. Chem. B* **2005**, *109*, 10073.
(25) Brown, M. E. *J. Therm. Anal. Calorim.* **2005**, *82*, 665.
(26) Brown, M. E. *Introduction to thermal analysis: Techniques and applications*, 2nd ed.; Kluwer: Dordrecht, 2001; Chapter 10.
(27) Vyazovkin, S.; Wight, C. A. *Annu. Rev. Phys. Chem.* **1997**, *48*, 125.
(28) Sestak, J.; Berggren, G. *Thermochim. Acta* **1971**, *3*, 1.
(29) Yang, J.; McCoy, B. J.; Madras, G. *J. Phys. Chem. B* **2005**, *109*, 18550.
(30) Yang, J.; McCoy, B. J.; Madras, G. *J. Chem. Phys.* **2005**, *122*.
(31) Liu, J.; Wang, J. J.; Li, H. H.; Shen, D. Y.; Zhang, J. M.; Ozaki, Y.; Yan, S. K. *J. Phys. Chem. B* **2006**, *110*, 738.
(32) Burnham, A. K.; Weese, R. K.; Weeks, B. L. *J. Phys. Chem. B* **2004**, *108*, 19432.
(33) Graetz, J.; Reilly, J. J. *J. Phys. Chem. B* **2005**, *109*, 22181.
(34) Wang, S.; Gao, Q. Y.; Wang, J. C. *J. Phys. Chem. B* **2005**, *109*, 17281.
(35) Hromadova, M.; Sokolova, R.; Pospisil, L.; Fanelli, N. *J. Phys. Chem. B* **2006**, *110*, 4869.
(36) Wu, C. Z.; Wang, P.; Yao, X. D.; Liu, C.; Chen, D. M.; Lu, G. Q.; Cheng, H. M. *J. Phys. Chem. B* **2005**, *109*, 22217.
(37) Peterson, V. K.; Neumann, D. A.; Livingston, R. A. *J. Phys. Chem. B* **2005**, *109*, 14449.
(38) Skrdla, P. J.; Robertson, R. T. *J. Phys. Chem. B* **2005**, *109*, 10611.
(39) Boldyrev, V. V. *Thermochim. Acta* **1986**, *100*, 315.
(40) Bagdassarian, C. *Acta Physicochim. U.S.S.R.* **1945**, *20*, 441.
(41) Allnatt, A. R.; Jacobs, P. W. M. *Can. J. Chem.* **1968**, *46*, 111.

(42) Guo, L.; Radisic, A.; Searson, P. C. *J. Phys. Chem. B* **2005**, *109*, 24008.
(43) Avrami, M. *J. Chem. Phys.* **1939**, *7*, 1103.
(44) Avrami, M. *J. Chem. Phys.* **1940**, *8*, 212.
(45) Erofeyev, B. V. *Dokl. Akad. Nauk SSSR* **1946**, *52*, 511.
(46) Jacobs, P. W. M. *J. Phys. Chem. B* **1997**, *101*, 10086.
(47) Prout, E. G.; Tompkins, F. C. *Trans. Faraday Soc.* **1944**, *40*, 488.
(48) Carstensen, J. T. *Drug stability: Principles and practices*, 2nd revised ed.; Marcel Dekker: New York, 1995; p. 237.
(49) Brown, M. E.; Glass, B. D. *Int. J. Pharm.* **1999**, *190*, 129.
(50) Brown, M. E. *Thermochim. Acta* **1997**, *300*, 93.
(51) Prout, E. G.; Tompkins, F. C. *Trans. Faraday Soc.* **1946**, *42*, 468.
(52) Skrdla, P. J. *J. Phys. Chem. A* **2004**, *108*, 6709.
(53) Guinesi, L. S.; Ribeiro, C. A.; Crespi, M. S.; Santos, A. F.; Capela, M. V. *J. Therm. Anal. Calorim.* **2006**, in press.
(54) Carstensen, J. T. *J. Pharm. Sci.* **1974**, *63*, 1.
(55) Chunxiu, G.; Yufang, S.; Donghua, C. *J. Therm. Anal. Calorim.* **2004**, *76*, 203.
(56) Liqing, L.; Donghua, C. *J. Therm. Anal. Calorim.* **2004**, *78*, 283.
(57) Gao, Z. M.; Amasaki, I.; Nakada, M. *Thermochim. Acta* **2002**, *385*, 95.
(58) Koga, N.; Criado, J. M. *J. Am. Ceram. Soc.* **1998**, *81*, 2901.
(59) Koga, N.; Criado, J. M. *J. Therm. Anal.* **1997**, *49*, 1477.
(60) Welch, A. J. E. Solid−solid reactions. In *Chemistry of the solid state*; Garner, W. E., Ed.; Academic Press: New York, 1955; Chapter 12.
(61) Wyandt, C. M.; Flanagan, D. R. *Thermochim. Acta* **1992**, *196*, 379.
(62) Booth, F. *Trans. Faraday Soc.* **1948**, *44*, 796.
(63) Jander, W. *Z. Anorg. Allg. Chem.* **1927**, *163*, 1.
(64) Ginstling, A. M.; Brounshtein, B. I. *J. Appl. Chem. USSR* **1950**, *23*, 1327.
(65) Crank, J. *The mathematics of diffusion*, 2nd ed.; Clarendon Press: Oxford, England, 1975; Chapter 6, p 89.
(66) Buscaglia, V.; Milanese, C. *J. Phys. Chem. B* **2005**, *109*, 18475.
(67) Eames, D. J.; Empie, H. J. International Chemical Recovery Conference: Changing Recovery Technology to Meet the Challenges of the Pulp and Paper Industry, Whistler, BC, Canada, June 11−14, 2001.
(68) Crank, J. *The mathematics of diffusion*, 2nd ed.; Clarendon Press: Oxford, England, 1975; Chapter 5, p 69.
(69) Perez-Maqueda, L. A.; Criado, J. M.; Malek, J. *J. Non-Cryst. Solids* **2003**, *320*, 84.
(70) Mampel, K. L. *Z. Phys. Chem.* **1940**, *A187*, 43.
(71) Mampel, K. L. *Z. Phys. Chem.* **1940**, *A187*, 235.
(72) Lopes, W. S.; Morais, C. R. D.; de Souza, A. G.; Leite, V. D. *J. Therm. Anal. Calorim.* **2005**, *79*, 343.
(73) Pap, A. E.; Kordas, K.; George, T. F.; Leppavuori, S. *J. Phys. Chem. B* **2004**, *108*, 12744.
(74) Carniti, P.; Gervasini, A.; Bennici, S. *J. Phys. Chem. B* **2005**, *109*, 1528.